Supplementary information

Copper(I) iodide based on $[Cu_5I_7]^{2-}$ unit and cationic organic ligands for X-ray scintillation and imaging

Qian Wu,[1] *Zhen-Zhong Lu,*[1]* *Rui Zhang*[2]

[1] State Key Laboratory of Flexible Electronics (LoFE) & Institute of Advanced Materials (IAM), School of Flexible Electronics (Future Technologies), Nanjing Tech University (NanjingTech), Nanjing 211816, China.

[2] School of Chemistry and Chemical Engineering, Suzhou University, Suzhou, Anhui 234000, China

Experimental and method

Synthesis of organic ligand Ted-Pre

The organic ligands Ted-Pre were synthesized following reported methods with minor modification.[1,2] Triethylenediamine (2.8 g, 25 mmol) was dissolved in anhydrous THF (50 mL). At room temperature, 3-bromopropene (2.41 g, 20 mmol) was added dropwise to the solution with stirring, controlling the dropping rate to avoid vigorous exothermic reaction. The formation of a white precipitate was observed immediately during the addition. After the addition was complete, the reaction mixture was stirred for an additional 2 hours. The precipitate was then collected by filtration, washed with acetone (3 × 25 mL), and dried under vacuum at 50 °C for 12 hours to afford the product as a white powder (2.8 g, yield 75%).^{1}H NMR (400 MHz, D_2O) δ 5.99 (m, 1H), 5.71 (m, 2H), 3.89 (d, J = 7.4 Hz, 2H), 3.41 (t, J = 7.6 Hz, 6H), 3.19 (t, J = 7.6 Hz, 6H).

Synthesis of organic ligand Ted-EA

The organic ligands Ted-EA were synthesized following reported methods with minor modification.[3] Triethylenediamine (2.24 g, 20 mmol) was dissolved in ethyl acetate (50 mL). At room temperature, ethyl bromoacetate (3.34 g, 20 mmol) was added dropwise to the solution with stirring, and the addition rate was controlled to prevent a vigorous reaction. The formation of a white precipitate was observed immediately during the addition. After the addition was complete, the reaction mixture was stirred for an additional 2 hours. The precipitate was then collected by filtration, washed with ethyl acetate (3 × 10 mL), and dried under vacuum at 50 °C for 12 hours to afford the product as a white powder (3.7 g, yield 66%). ^{1}H NMR (400 MHz, $CDCl_3$) δ 4.94 (s,

2H), 4.22 (q, *J* = 7.2 Hz, 2H), 4.06 (t, *J* = 7.6 Hz, 6H), 3.21 (t, *J* = 7.6 Hz, 6H), 1.27 (t, *J* = 7.2 Hz, 3H).

Synthesis of single crystals of 1

CuI (19 mg, 0.1 mmol) was dissolved in 2 mL acetonitrile. Then, the organic ligand Ted-Pre (38 mg, 0.2 mmol) was dissolved in a mixed solvent of DMF and H_2O (2 mL, 1:1, v:v). The two solutions were combined and transferred into a 25 mL autoclave lined with polytetrafluoroethylene, which was then sealed and heated at 50 °C for 48 hours, resulting in a light-yellow clear solution. Transparent needle-like crystals were obtained after standing at room temperature for approximately 4 days, which were collected by filtration and washed with acetonitrile. The yield was 35% based on ligand. Elemental analysis (%) for **1**, $C_{21}H_{43}Cu_5I_7N_5O_2$. Calcd: C, 15.73; H, 2.70; N, 4.37. Found: C, 15.91; H, 2.58; N, 4.31.

Synthesis of single crystals of 2

CuI (38 mg, 0.2 mmol) was dissolved in 2 mL saturated aqueous solution of KI, and the resulting solution was placed at the bottom of a test tube. Then, a methanol solution (2 mL) containing organic ligand Ted-EA (14 mg, 0.1 mmol) was slowly added dropwise onto the CuI solution, forming distinct liquid layers within the test tube. After standing at room temperature for 48 hours, transparent needle-like crystals were obtained, which were collected by filtration and washed with methanol. The yield was 86% based on ligand. Elemental analysis (%) for **2**, $C_{20}H_{42}Cu_5I_7N_4O_6$. Calcd: C, 14.64; H, 2.58; N, 3.41. Found: C, 14.72; H, 2.49; N, 3.38.

Fabrication of composite film

The crystals of **1** were ground thoroughly using a mortar and passed through a 200-mesh sieve to obtain uniform fine powder. The powder of **1** (30 mg) was mixed with 200 mg of polydimethylsiloxane (PDMS) and ultrasonicated for 30 minutes to ensure homogeneous dispersion of the CP powder. Subsequently, 20 mg of curing agent was added and stirred for 5 minutes. The resulting mixture was drop-cast onto a polytetrafluoroethylene (PTFE) mold and spin-coated to form a uniform film. The film was then cured at 120 °C for 150 minutes. After naturally cooling to room temperature, the flexible scintillating film was peeled off from the PTFE substrate.

X-ray excited luminescence (XEL) spectra collection

The XEL spectra were measured by using a commercial miniature X-ray source, combined with an Edinburgh FS5 fluorescence spectrophotometer (Edinburgh Instruments Ltd.). The X-ray source was a commercial miniature silver (Ag) target X-ray tube (AMPTEK, Inc.), with a maximum tube current/power light output of 80 μA/4W.

Calculation of the X-ray attenuation efficiency.

The X-ray attenuation efficiency (AE) was calculated using the following equation:

$$AE(\varepsilon,d) = \left(1 - e^{-c(\varepsilon)\rho d}\right) \times 100\%$$

Where $c(\varepsilon)$ is the photon cross-section function obtained from the NIST XCOM database, ε is the corresponding photon energy, ρ is the density of the scintillator, and d is the thickness. The densities of the commercial BGO and anthracene crystals utilized were 7.13 g/cm^3 and 1.24 g/cm^3, respectively. In this study, we used a quartz

sample cell containing 10 × 16 × 2 mm groove. The CP crystalline samples were packed in the groove for data collection. The density of **1** and **2** samples packed in the sample cell was calculated as 0.658 and 0.821 g/cm³, respectively. For the calculation of the relationship between attenuation efficiency and scintillator thickness, we used a photon energy of 22 keV (the average energy of the X-ray tube) and a thickness of 2 mm. The mass absorption coefficients of BGO, anthracene, **1**, and **2** were 54.30, 0.395, 15.61, and 15.32 cm^2/g, respectively (Figure 5a in the main text). As shown in Figure S6, the attenuation efficiencies of BGO, anthracene, **1**, and **2** calculated by the above equation are 100%, 9.329%, 87.19% and 91.92%.

Calculation of relative light yield (LY).

The relative light yield under X-ray excitation is determined using the method described in the literature,[1]

$$PC_{normalized} = \frac{PC_{measured}}{AE(\varepsilon,d)}$$

$$LY_{sample} = LY_{reference}\frac{PC_{normalized}(sample)}{PC_{norealized}(reference)}$$

Where AE(d) is the attenuation coefficient at the actual thickness, $LY_{reference}$ is the light yield of BGO (10000 photons MeV^{-1}),[2] PC (Photon Counting) is obtained as the integral area of the XEL peaks for the sample.

The XEL spectra for BGO, **1**, and **2** were collected and shown in Figure 5b in the main text. The integral areas of XEL peaks for each material were 863421, 1433180 and 961073 for BGO, **1**, and **2**, respectively. Then the relative light yield for **1** was obtained:

$$LY_{CP3=} 10000 \times \frac{1433180 / 87.19\%}{863421 / 100\%}$$ MeV^{-1} ≈ 19010 photons MeV^{-1}

Using the same equation, the relative light yield for **2** was 12110 photons MeV^{-1}.

Calculation of limit of detection (LOD).

The detection limit can be calculated according to the following equation:

$$LOD = \frac{3\sigma}{slope}$$

where σ is the instrumental average noise and slope is the slope of the fitted line. Through the measurement of dose-dependent XEL spectra, a linear correlation was observed between XEL intensity and dose rate with the slope of this correlation representing the sensitivity of the X-ray detector. Subsequently, the background noise was assessed under the condition where the scintillator was positioned in the sample cell without X-ray exposure, so as to determine the signal-to-noise ratio (SNR). Then, the detection limit of the system was calculated using above equation.

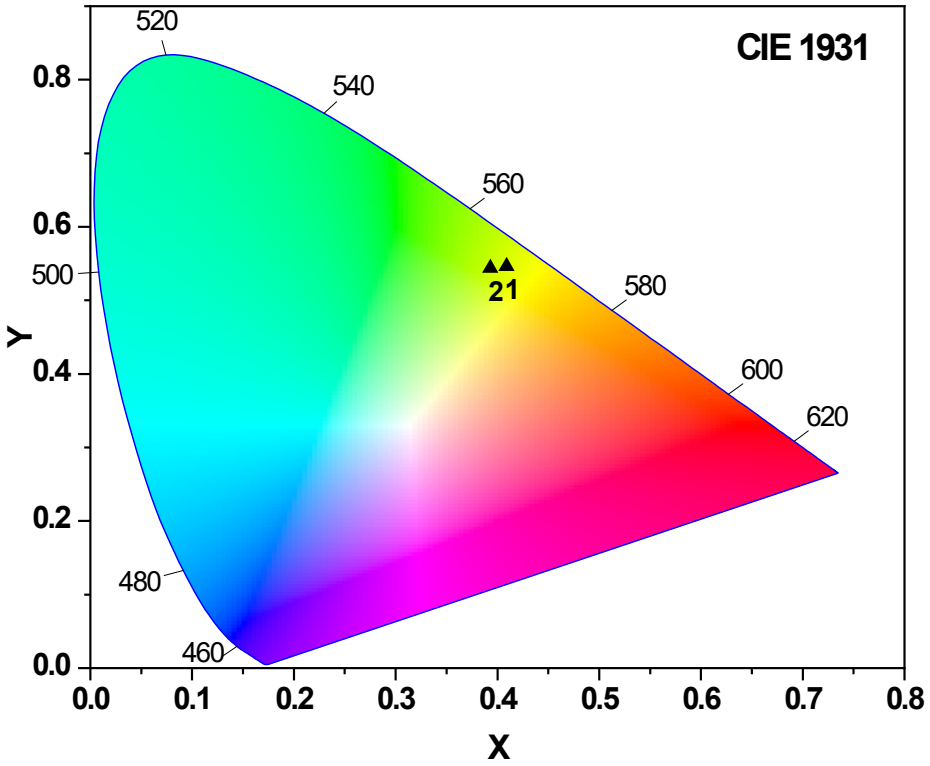

Figure S1. The CIE coordinates for **1** and **2**.

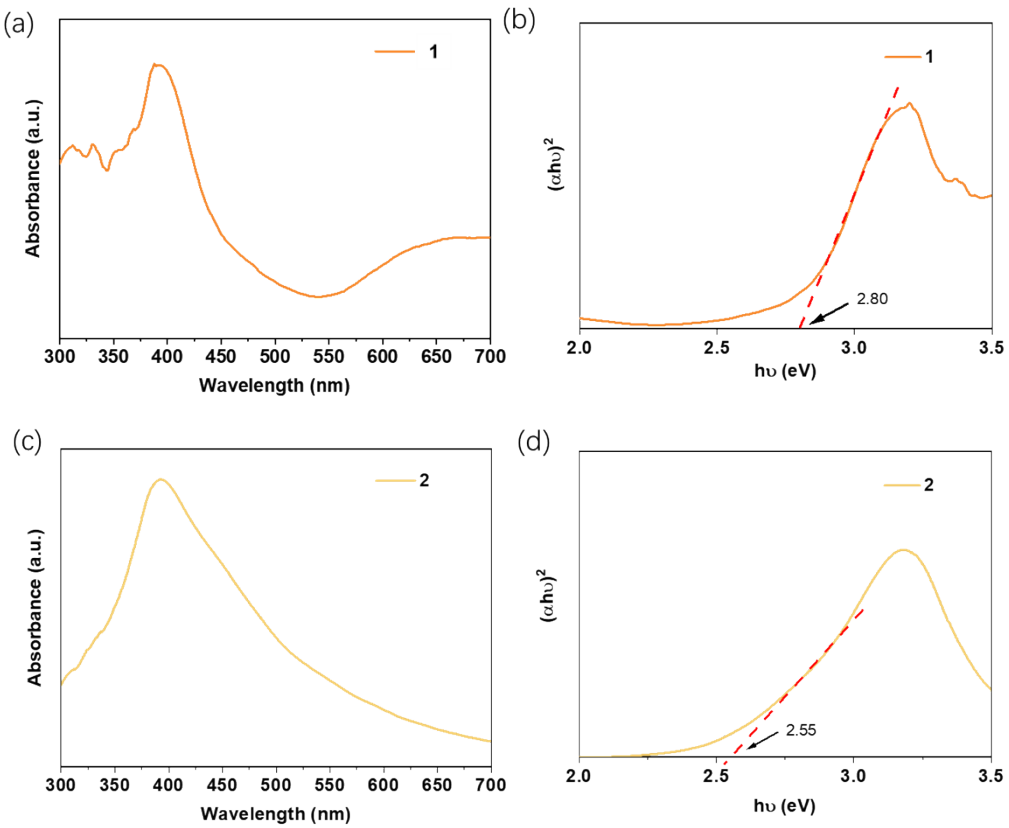

Figure S2. UV-Vis spectra for **1** and **2**.

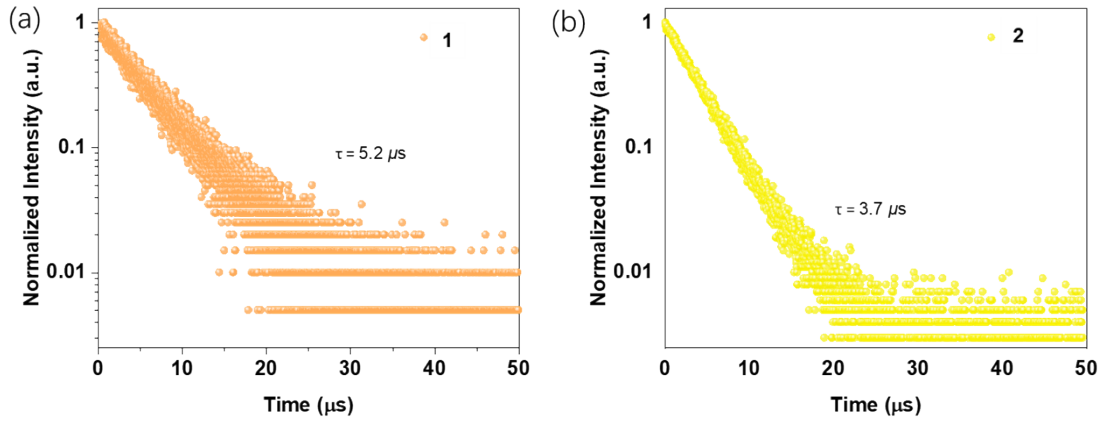

Figure S3 The lifetime decay curves of **1** and **2**.

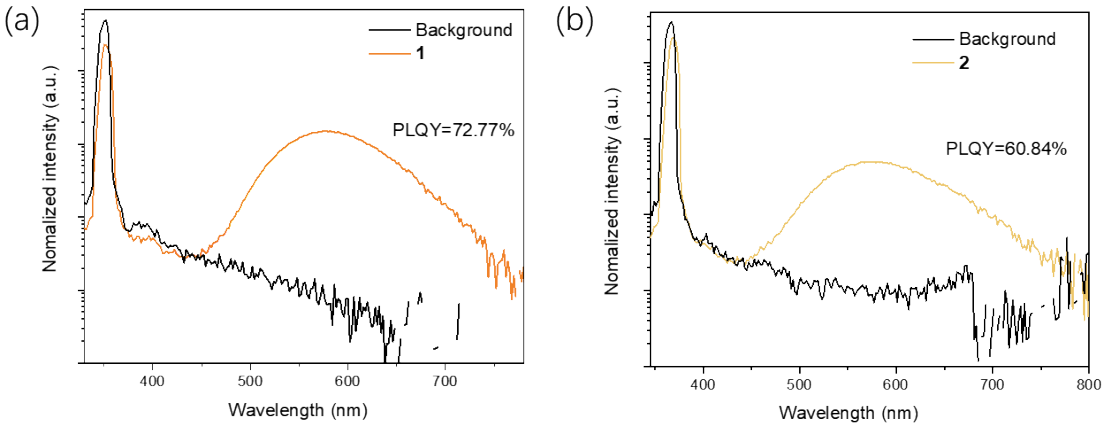

Figure S4. Photoluminescent quantum yield analysis curves of **1** and **2**.

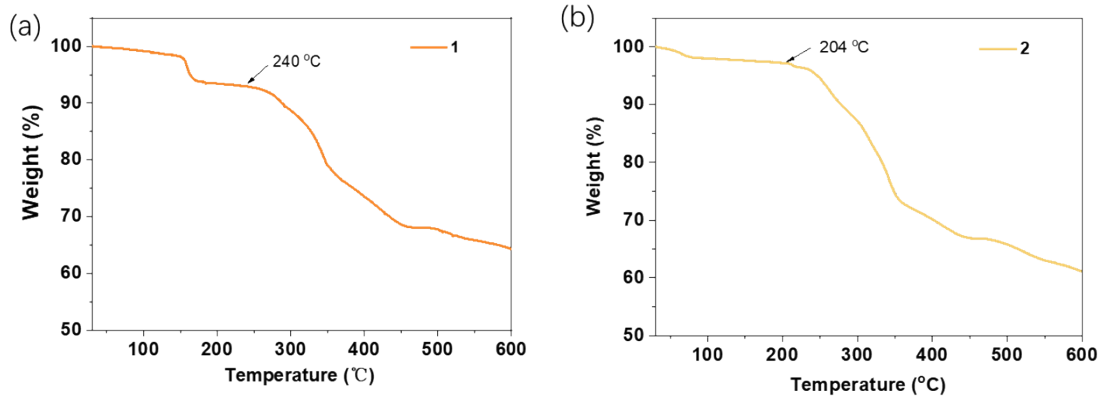

Figure S5. The thermal gravimetric profiles for **1** and **2**.

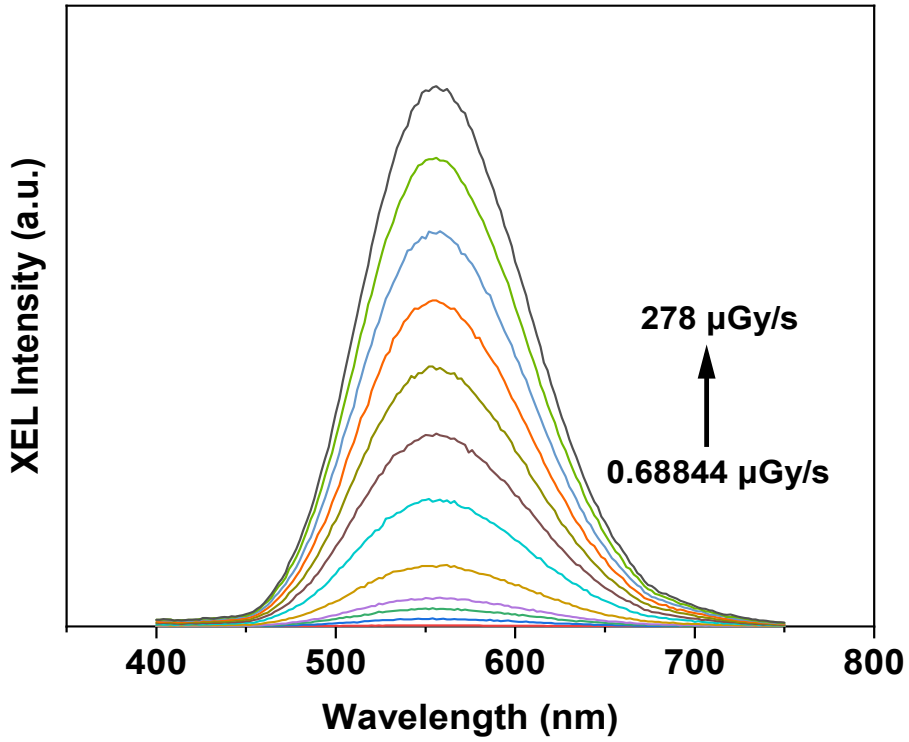

Figures S6. The XEL intensity spectra of **2** with the increase of X-ray dose rate.

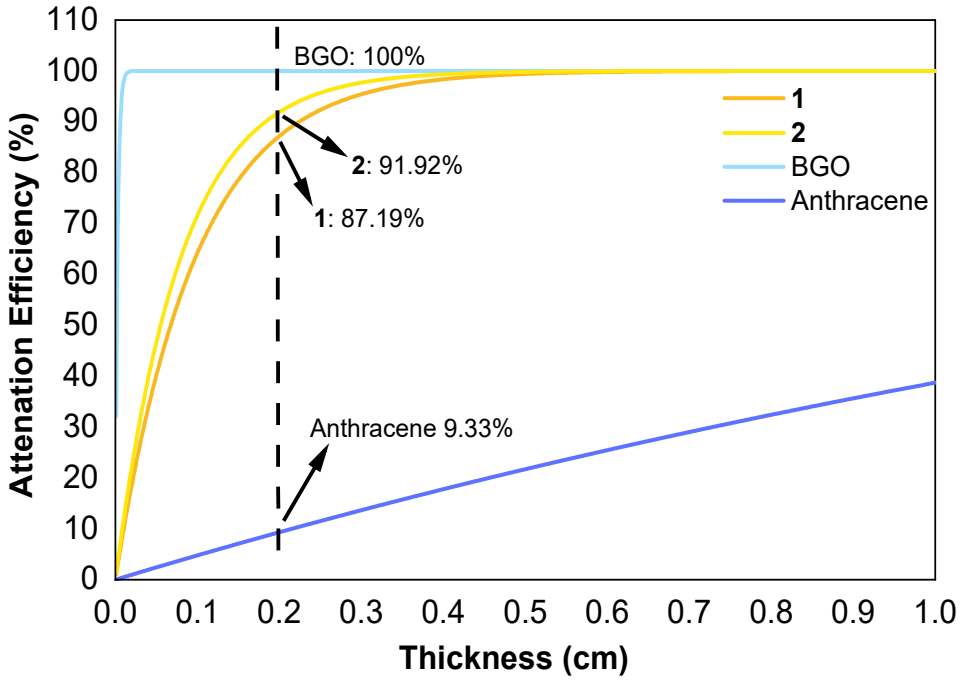

Figure. S7. The attenuation efficiency curve of **1**, **2**, BGO and anthracene

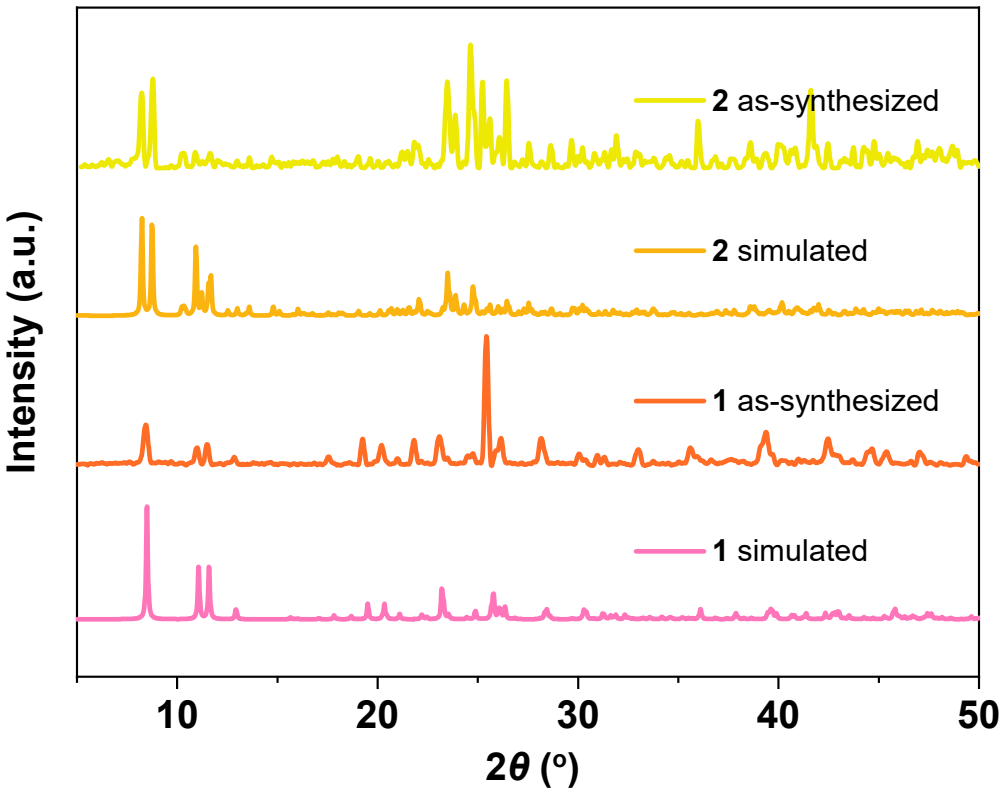

Figure S8. Powder X-ray diffraction profiles for **1** and **2**.

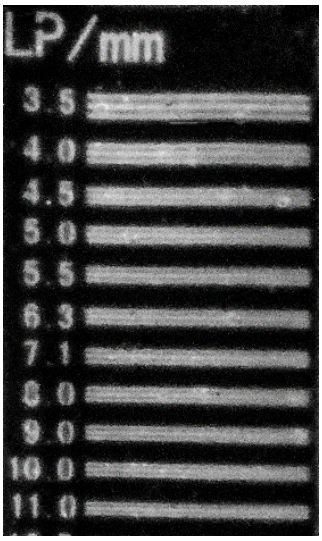

Figure S9. X-ray images of line-pair-card for the scintillation film of complex **1**.

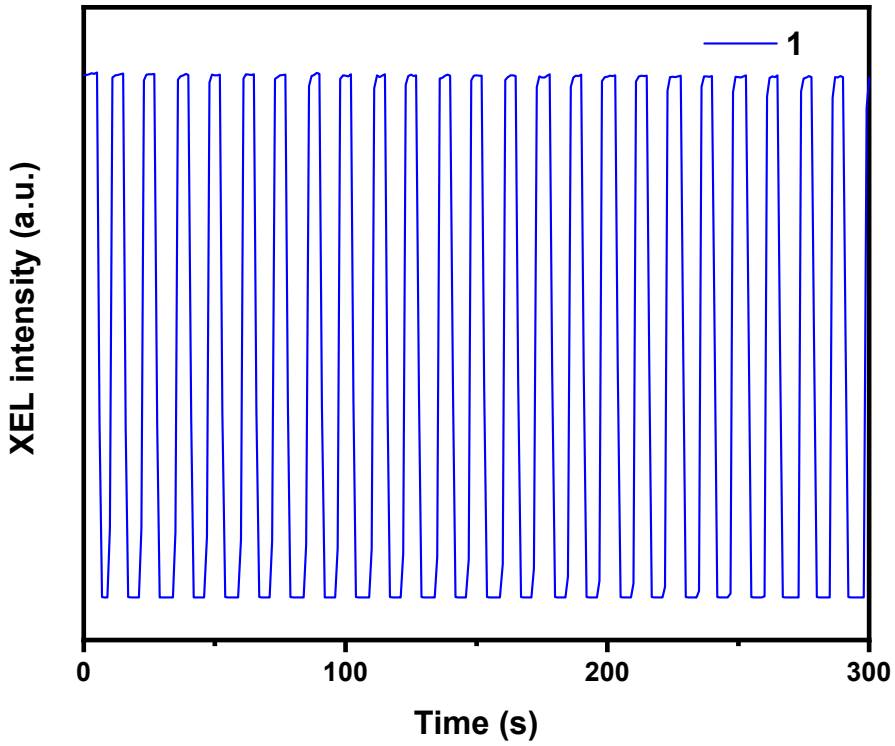

Figure S10. X-ray excited luminescence stability of **1** under on-off cycles of X-ray at a dose rate of 278 μGy s^{-1}.

Table S1. Summary of crystal data of **1** and **2**.

Compound	**1**	**2**
Empirical formula	$C_{21}H_{43}Cu_5I_7N_5O_2$	$C_{20}H_{42}Cu_5I_7N_4O_6$
Formula weight	1603.60	1640.57
Temp. (K)	223	223
Radiation type	MoKα	CuK\a
Diffrn. wavelength (Å)	0.71073	1.54178
Crystal system	monoclinic	triclinic
Space group	C m	P-1
a (Å)	15.107(1)	8.869(1)
b (Å)	16.010(1)	11.628(1)
c (Å)	8.814(1)	21.022(1)
α (°)	90	105.20(1)
β (°)	115.038(3)	90.63(1)
γ (°)	90	106.35(1)
V (Å^3)	1931.6(3)	1999.3(3)
Z	2	2
ρ_{calc} Mg/m^3	2.757	2.725
F(000)	1472	1508
Refl. collected	29311	21555
Final R indexes(R_1)	0.0287	0.0498
(all data) wR_2	0.0782	0.1453
GOOF	1.064	1.006

Table S2. The selected bond lengths for **1** and **2**

Compound	Atom–Atom	Length [Å]	Atom–Atom	Length [Å]
1	I1-Cu2	2.652(2)	I4-Cu3	2.533(1)
	I1-Cu3	2.739(2)	I4-Cu3	2.533(1)
	I1-Cu3	2.739(2)	I5-Cu1	2.703(1)
	I2-Cu1	2.575(1)	I5-Cu1	2.703(1)
	I2-Cu2	2.636(1)	I5-Cu2	2.844(2)
	I3-Cu1	2.629(1)	I5-Cu3	3.027(2)
	I3-Cu3	2.511(1)	I5-Cu3	3.027(2)
	Cu1–N1	2.141(8)		
	Cu3–Cu3#1	2.510(3)	Cu1–Cu3	2.731(2)
	Cu1–Cu2	2.794(1)		
2	I5–Cu5	2.611(1)	I3–Cu3	2.618(1)
	I5–Cu1	2.515(1)	I3–Cu4	2.659(1)
	I2–Cu3	2.629(1)	I1–Cu1	2.606(1)
	I2–Cu2	2.504(1)	I1–Cu2	2.591(2)
	I6–Cu5	2.681(1)	I4–Cu4	2.684(1)
	I6–Cu4	2.696(1)	I7–Cu1	2.636(2)
	I6–Cu2	2.647(2)	I4–Cu5	2.621(1)
	I7–Cu3	2.724(1)	I7–Cu4	2.685(1)
	Cu4-N3	2.139(7)	Cu5-N2	2.149(7)
	Cu2–Cu3	2.524(2)	Cu1-Cu4	2.760(2)
	Cu2–Cu5	2.790(2)	Cu1-Cu5	2.850(2)
	Cu3-Cu4	2.856(3)		

Table S3 Summary of recently reported CuI complexes based on Ted-modified ligands.

Formula	Organic ligand	Cu-Cu distance (Å)	PL λ_{em}	PLQY	Relative Light yield / XEL intensity	Ref
$Cu_4I_6(Ted\text{-}Pr)_2$	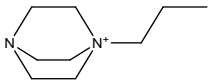	2.67	527	95.3%	32600	4
$Cu_4I_6(Ted\text{-}Pr)_2$	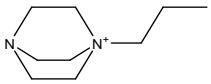	2.64, 2.70	527	97.1	- / 3.41 times BGO	5
$Cu_6I_8(Ted\text{-}Bu)_2$@SDBS	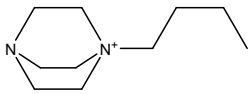	2.66, 2.71	530	100%	- / 4.80 times LuAG	6
$Cu_5I_7(Ted\text{-}Bz)_2$	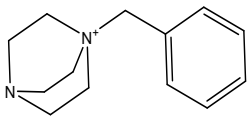	2.78	570	100%	38800	7
$Cu_5I_7(Ted\text{-}Pre)_2$	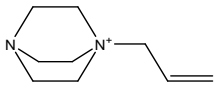	2.779	556	72.8%	19010	This work
$Cu_5I_7(Ted\text{-}EA)_2$	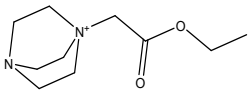	2.7562	552	60.8%	12110	This work

Reference

Reference

1 Karton-Lifshin, N.; Katalan, S.; Columbus, I.; Chen, R.; Yehezkel, L.; Madmon, M.; Dagan, S.; Elias, S.; Fridkin, G.; Zafrani, Y. Effective Neutralization of Chemical Warfare Agents (HD, VX) by Me-DABCOF: A Small Molecule with Dual Action. *Chem. Commun.* **2019**, 55, 12471–12474.

2 Maraš, N.; Polanc, S.; Kočevar, M. Ring-Opening Reactions of 1,4-Diazabicyclo[2.2.2]octane (DABCO) Derived Quaternary Ammonium Salts with Phenols and Related Nucleophiles. *Org. Biomol. Chem.* **2012**, 10, 1300–1310.

3 Zeng, R.; Shan, C.; Liu, M.; Jiang, K.; Ye, Y.; Liu, T.-Y.; Chen, Y.-C. [4+1+1] Annulations of α-Bromo Carbonyls and 1-Azadienes toward Fused Benzoazabeteocycles. *Org. Lett.* **2019**, 21, 2312–2316.

4 He, T.; Zhou, Y.; Yuan, P.; Yin, J.; Gutierrez-Arzaluz, L.; Chen, S.; Wang, J.-X.; Thomas, S.; Alshareef, H. N.; Bakr, O. M.; Mohammed, O. F. Copper Iodide Inks for High-Resolution X-ray Imaging Screens. *ACS Energy Lett.* **2023**, 8, 1362–1370.

5 Wang, Y.; Zhao, W.; Guo, Y.; Hu, W.; Peng, C.; Li, L.; Wei, Y.; Wu, Z.; Xu, W.; Li, X.; Suhe, Y. D.; Liu, X.; Huang, W. Efficient X-ray Luminescence Imaging with Ultrastable and Eco-Friendly Copper(I)-Iodide Cluster Microcubes. *Light: Sci. Appl.* **2023**, 12, 155.

6 Gu, R.; Han, K.; Jin, J.; Zhang, H.; Xia, Z. Surfactant-Assisted Synthesis of Hybrid Copper(I) Halide Nanocrystals for X-ray Scintillation Imaging. *Chem. Mater.* **2024**, 36, 2963–2970.

7 Liang, M.; Gang, K.; Li, L.; Liu, K.; Yan, D.; Wang, S.; Liu, S.; Liu, X.; Zhao, Q.; Zheng, K. Ligand-Engineered All-In-One Cu(I) Iodide Complex Enables Near-Unity Photoluminescence and Advanced 3D X-ray Image Reconstruction. *Angew. Chem. Int. Ed.* **2025**, 64, e202512471.